This copy of the ESI replaces the previous version published on 12 Jan 2022

# Electronic Supplementary Information for

# Predicting spike protein NTD mutations of SARS-CoV-2 causing immune escape by molecular dynamics simulations

Liping Zhou[a,b,#], Leyun Wu[a,b,#], Cheng Peng[a,b], Yanqing Yang[a,b], Yulong Shi[a,b], Likun Gong[b,c], Zhijian Xu[a,b,*], Weiliang Zhu[a,b,*]

[a]Drug Discovery and Design Center, Shanghai Institute of Materia Medica, Chinese Academy of Sciences, Shanghai, 201203, China

[b]School of Pharmacy, University of Chinese Academy of Sciences, No.19A Yuquan Road, Beijing, 100049, PR China

[c]Center for Drug Safety Evaluation and Research, Shanghai Institute of Materia Medica, Chinese Academy of Sciences, Shanghai 201203, China

[#] Liping Zhou and Leyun Wu contributed equally to this work.

[*]Corresponding Author

E-mail: zjxu@simm.ac.cn (Z.X.), wlzhu@simm.ac.cn (W.Z.).

ORCID:

Weiliang Zhu: 0000-0001-6699-5299

Zhijian Xu: 0000-0002-3063-8473

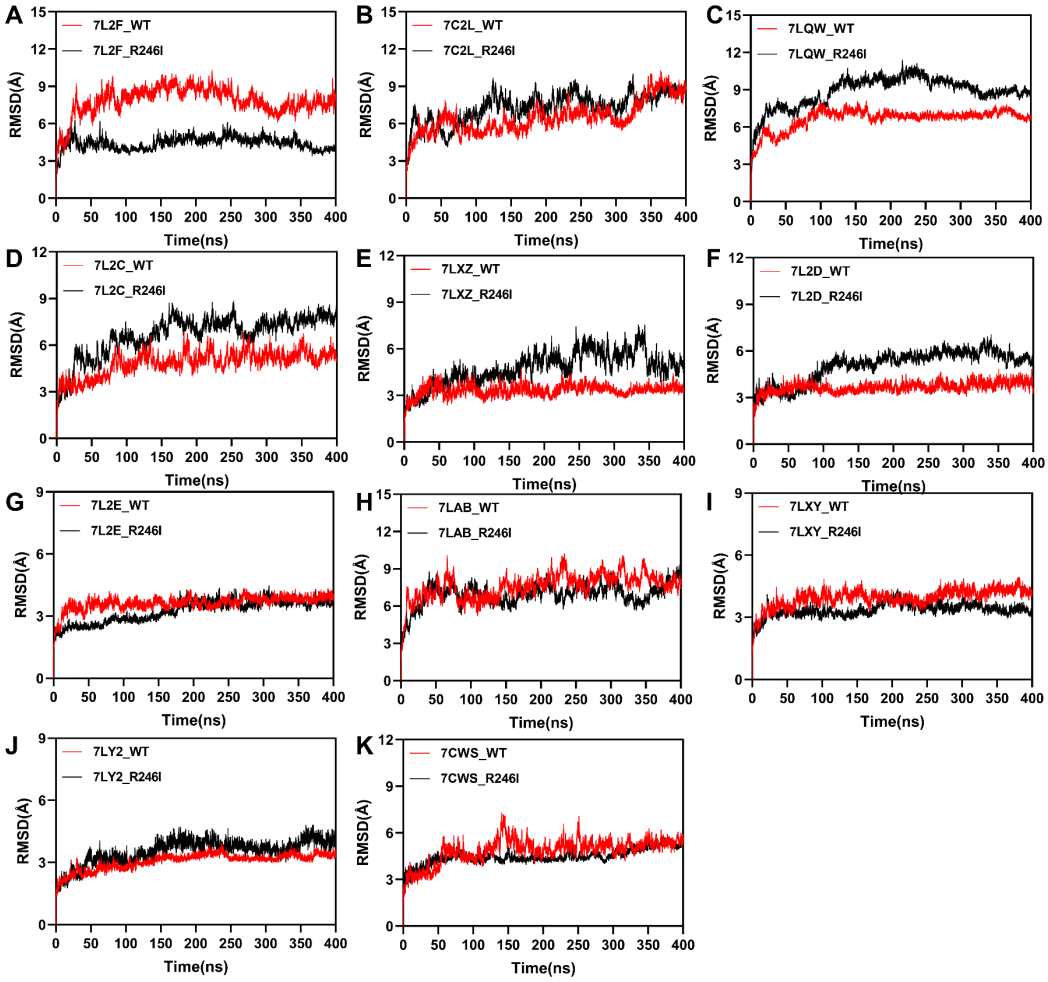


**Figure S1.** Time dependence of the heavy atom RMSD during 400 ns MD simulation for all systems. (A-K) RMSD for different systems including $NTD_{WT}$ or $NTD_{R246I}$ to antibodies 5-24 (PDB ID: 7L2F), 4A8 (PDB ID: 7C2L), 2-17 (PDB ID: 7LQW), 2-51 (PDB ID: 7L2C), S2L28 (PDB ID: 7LXZ), 1-87 (PDB ID: 7L2D), 4-18 (PDB ID:7L2E), DH1052 (PDB ID:7LAB), S2X333 (PDB ID:7LXY), S2M28 (PDB ID: 7LY2) and FC05 (PDB ID: 7CWS).

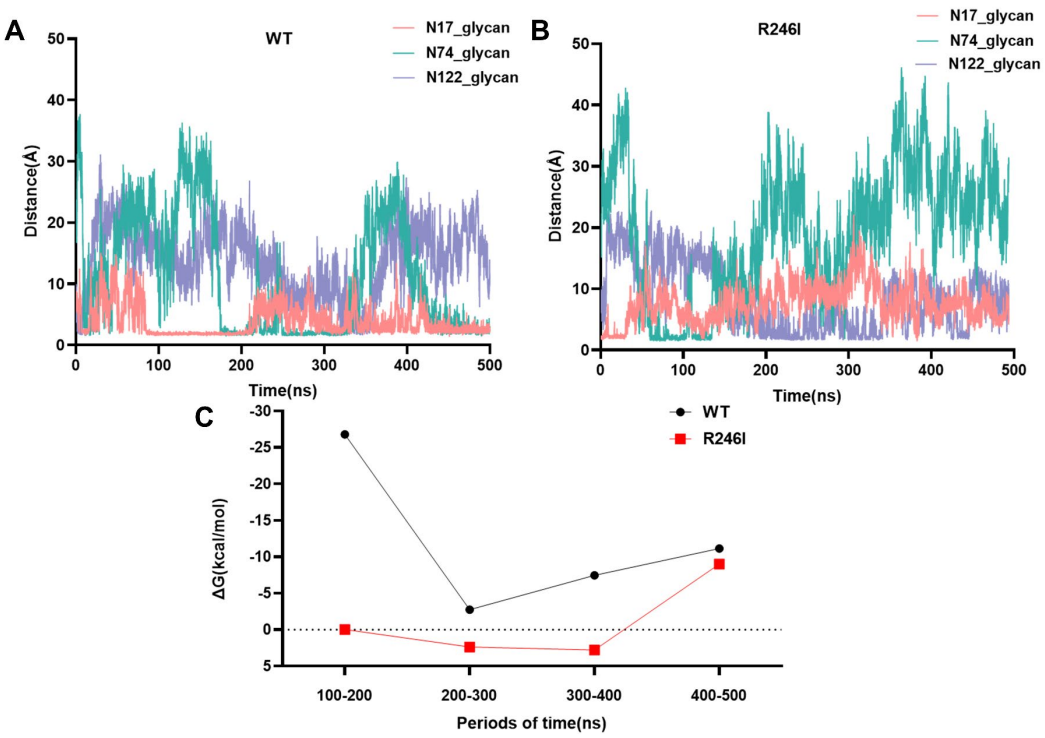


**Figure S2.** Glycans-antibody distance and the binding free energy contribution of glycans in NTD$_{WT}$ or NTD$_{R246I}$ system (PDB ID: 7L2F). (A-B) The minimum distances variation between N17, N74, N122 glycans of glyco-NTD$_{WT}$ or glyco-NTD$_{R246I}$ and antibody 5-24. (C) The binding free energy contribution of glycans calculated by MM/GBSA in different time periods.

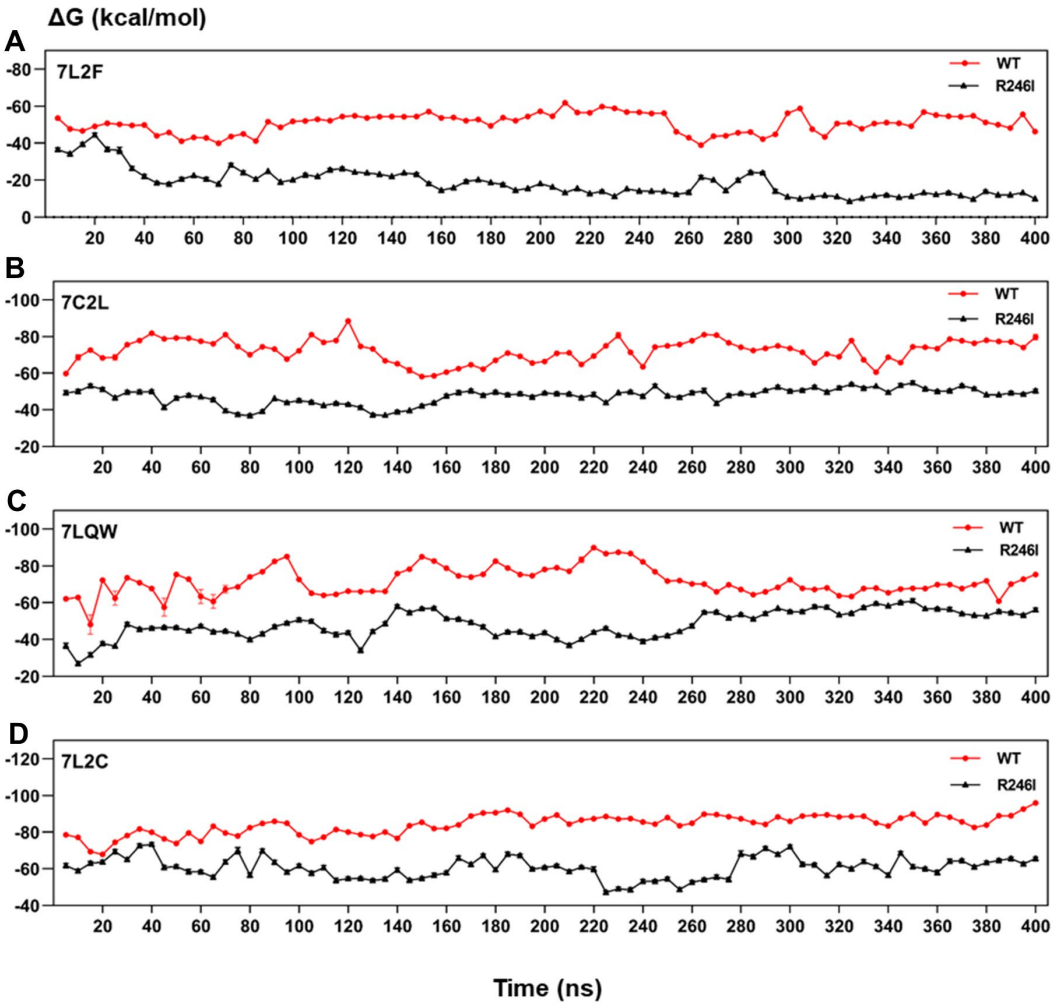


**Figure S3.** (A-D) The binding free energy change for $NTD_{WT}$ or $NTD_{R246I}$ to 4 mAbs, *viz* 5-24 (PDB ID: 7L2F), 4A8 (PDB ID: 7C2L), 2-17 (PDB ID: 7LQW), 2-51 (PDB ID: 7L2C). The binding free energy in WT is filled with red, and the binding free energy in R246I mutant is filled with black. Binding free energy calculations were executed every 5ns.

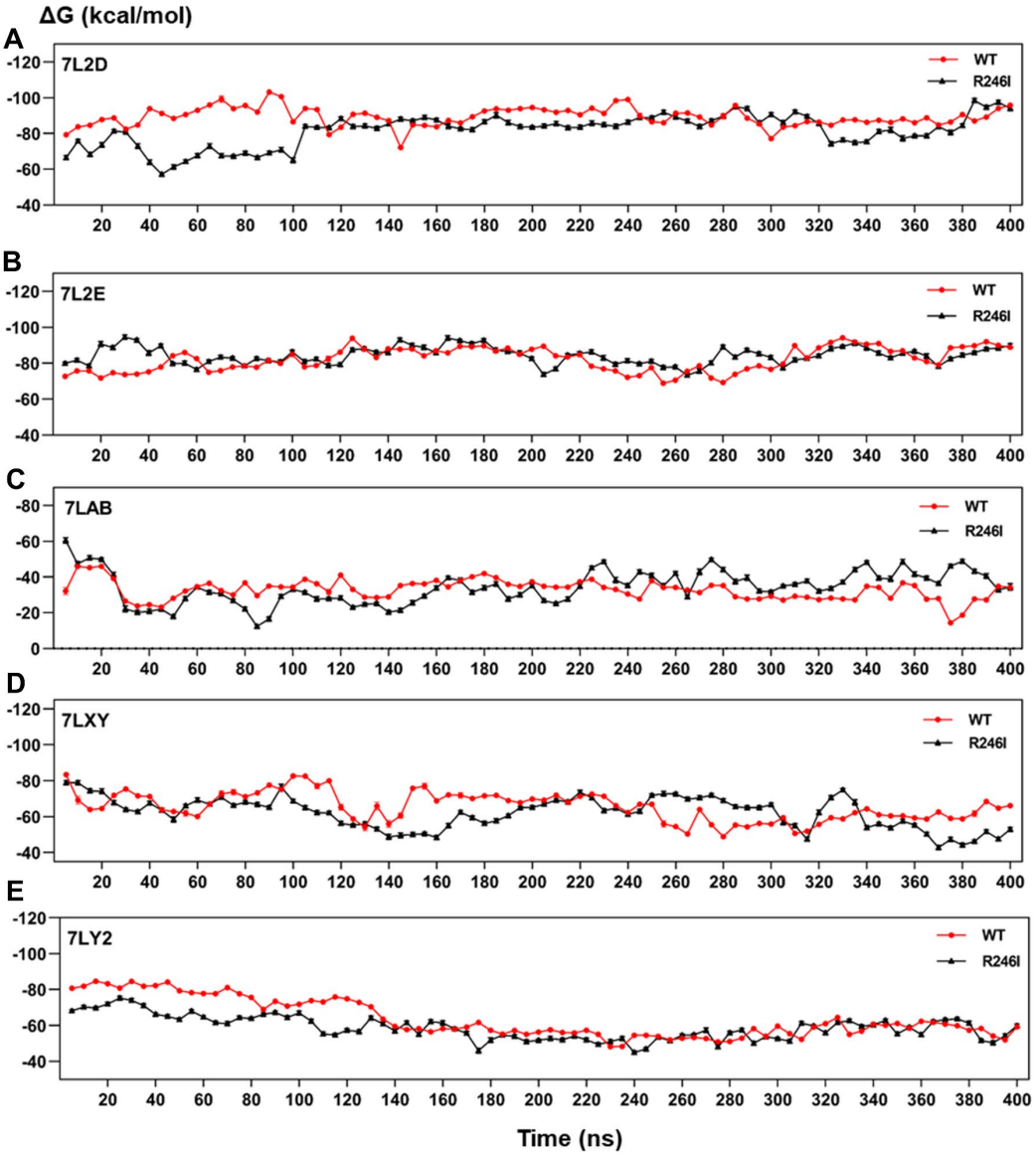


**Figure S4.** (A-E) The binding free energy change for $NTD_{WT}$ or $NTD_{R246I}$ to 5 mAbs, *viz* 1-87 (PDB ID: 7L2D), 4-18 (PDB ID:7L2E), DH1052 (PDB ID:7LAB), S2X333 (PDB ID:7LXY) and S2M28 (PDB ID: 7LY2). The binding free energy in WT is filled with red, and the binding free energy in R246I mutant is filled with black. Binding free energy calculations were executed every 5ns.

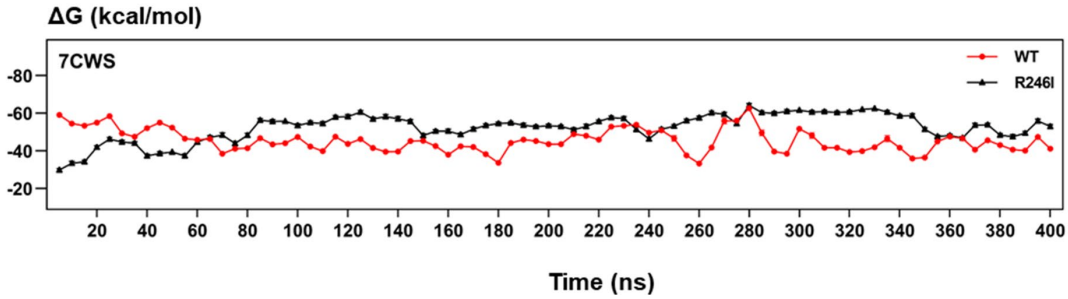


**Figure S5.** The binding free energy change for $NTD_{WT}$ or $NTD_{R246I}$ to FC05 (PDB ID: 7CWS). The binding free energy in WT is filled with red, and the binding free energy in R246I mutant is filled with black. Binding free energy calculations were executed every 5ns.

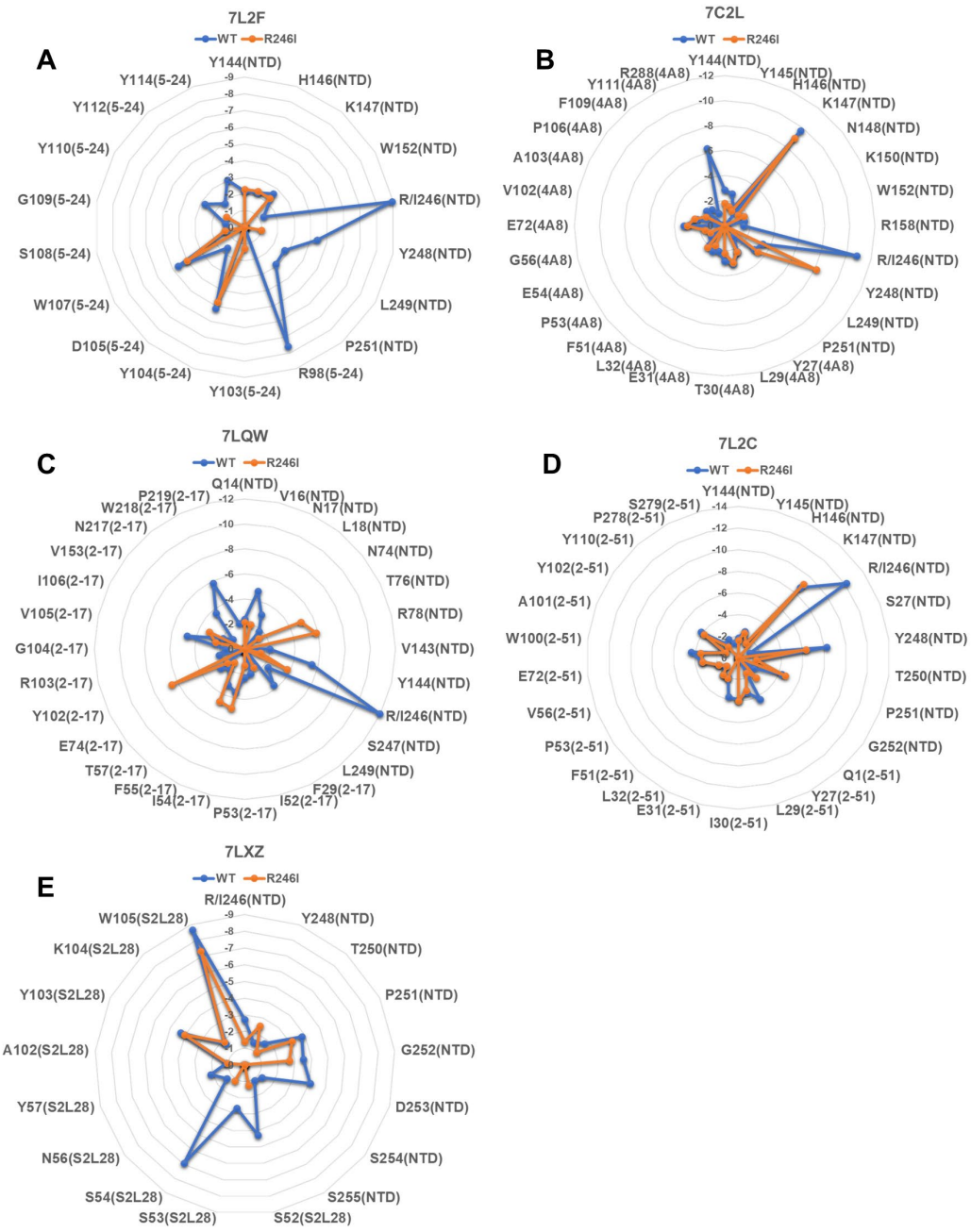


**Figure S6.** (A-E) The energy decomposition for per residue in 5 systems (kcal/mol). Residues whose energy contribution < -1.00 kcal/mol are shown here. The antibody names or NTD are in the parentheses.

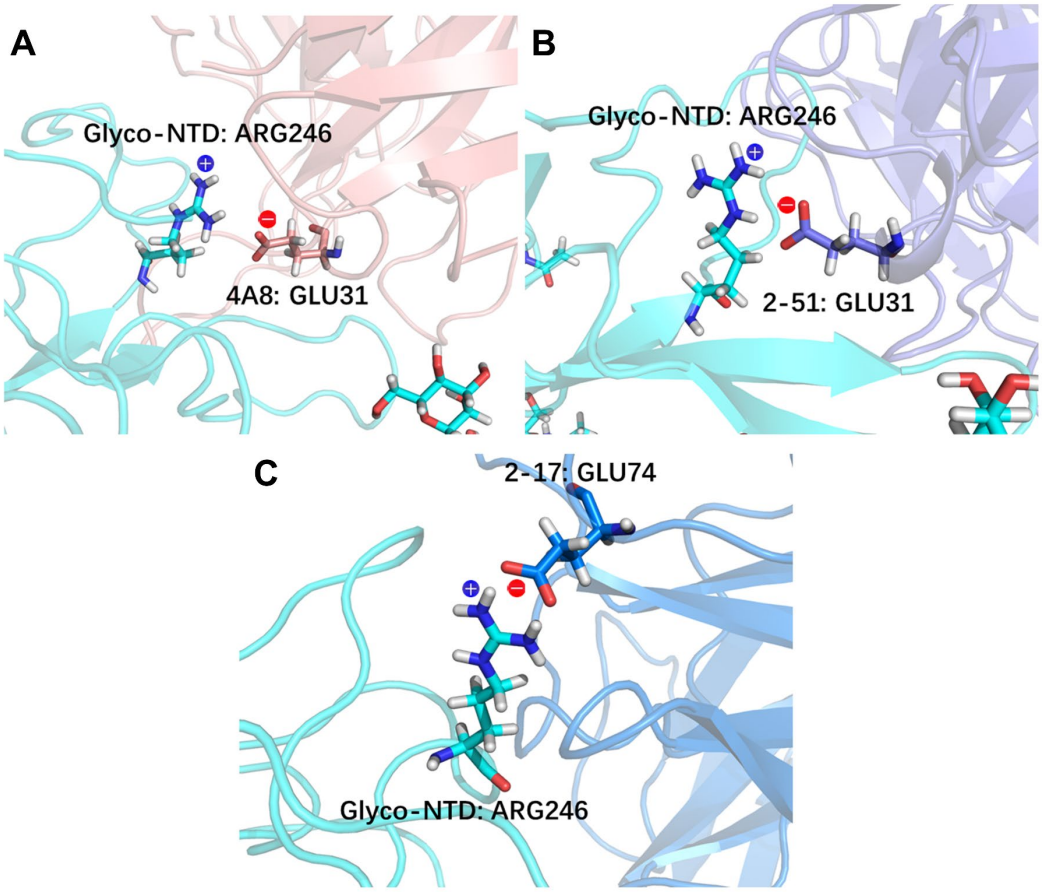


**Figure S7.** Three types of glycosylated $NTD_{WT}$-mAb binding modes. The blue circular icon represents positive charge and the red one is negative charge. (A) Interactions of R246 (cyan) belonging to NTD and E31 belonging to antibody 4A8 (salmon) (PDB ID: 7C2L). (B) Interactions of R246 (cyan) belonging to NTD and E31 belonging to antibody 2-51 (slate) (PDB ID: 7L2C). (C) Interactions of R246 (cyan) belonging to NTD and E74 belonging to antibody 2-17 (marine) (PDB ID: 7LQW).

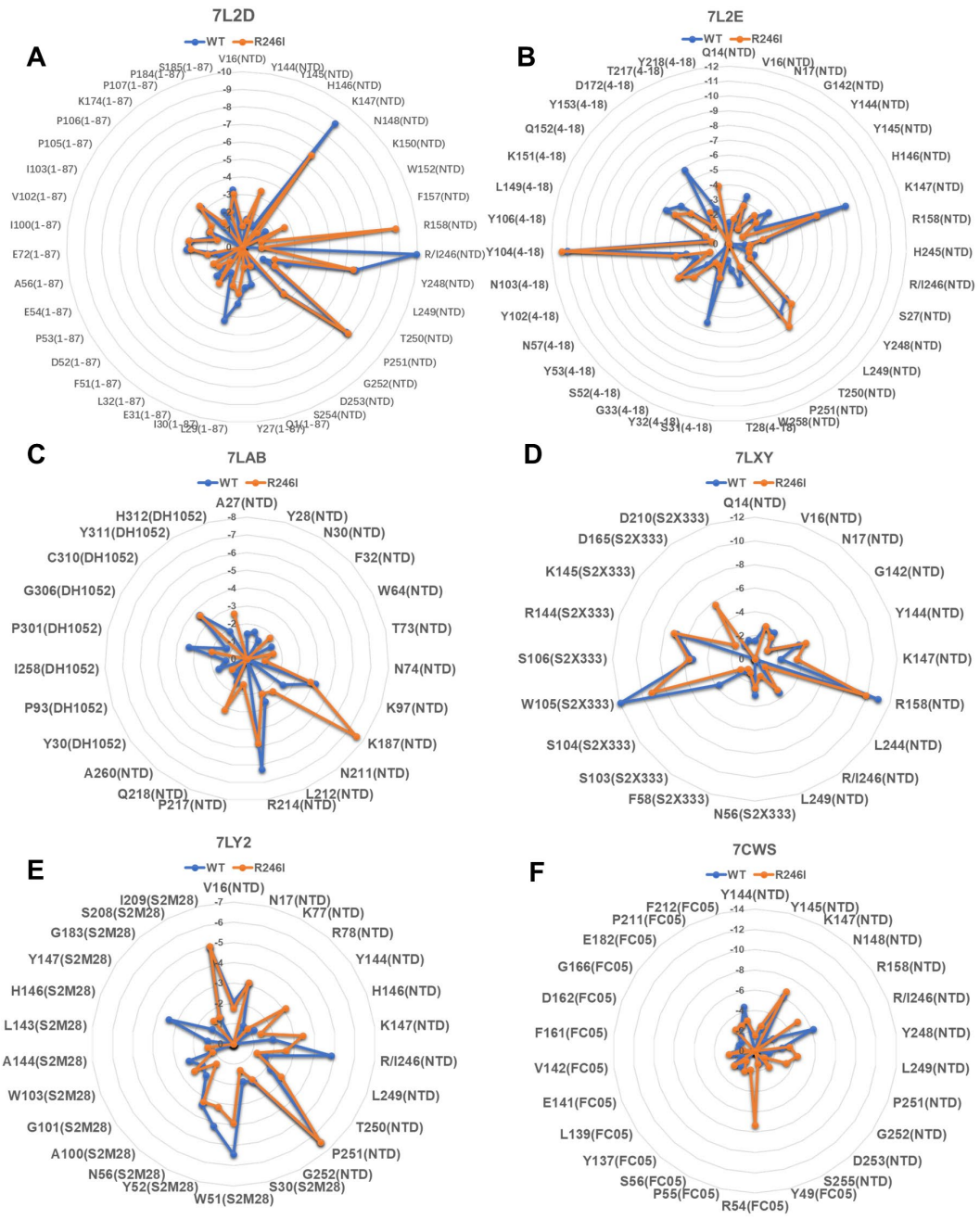


**Figure S8.** (A-F) The energy decomposition for per residue in 6 systems (kcal/mol). Residues whose energy contribution < -1.00 kcal/mol are shown here. The antibody names or NTD are in the parentheses.

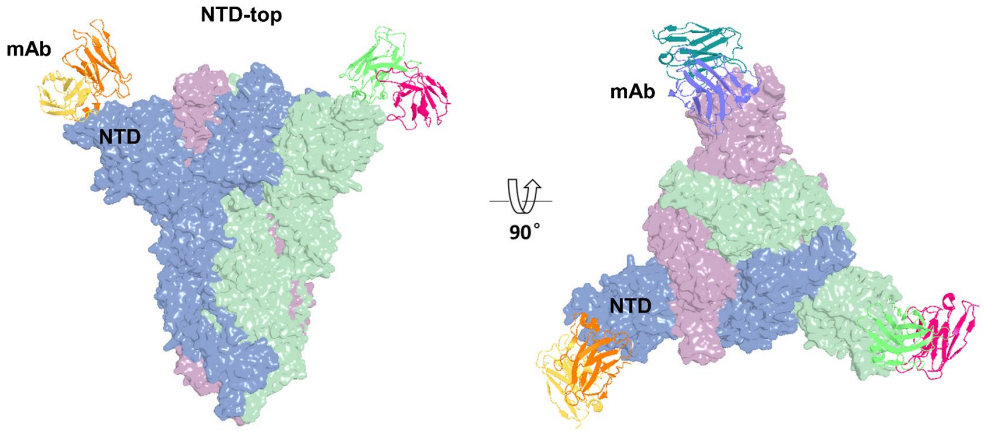


**Figure S9.** Structure-based mapping of mAbs binding to S protein trimer in NTD-top mode. Chains A, B and C of spike protein are depicted with surface, and mAbs are shown in cartoon representation.

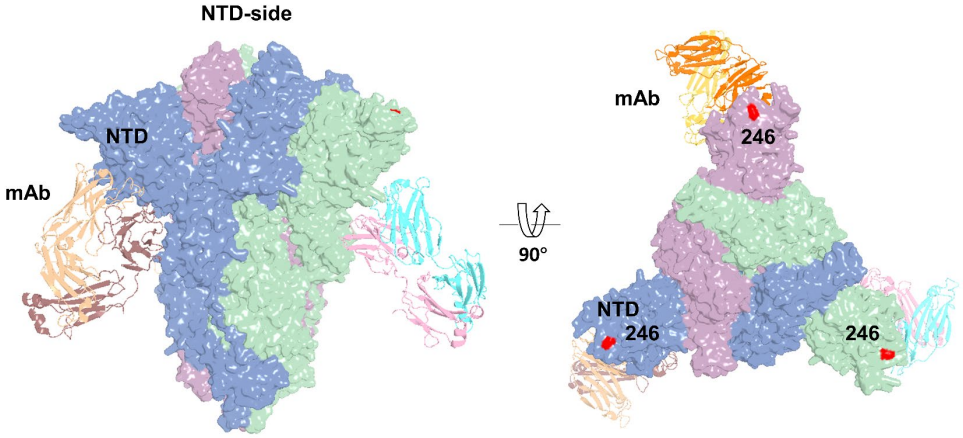


**Figure S10.** Structure-based mapping of mAbs binding to S protein trimer in NTD-side mode. Chains A, B and C of spike protein are depicted with surface, and mAbs are shown in cartoon representation. The positions of residue 246 on NTD is colored by red.

This copy of the ESI replaces the previous version published on 12 Jan 2022

**Table S1.** The glycosylation of NTD according to experimental data[1,2]

| Residues | Type | Glycan |
|---|---|---|
| N17A | FA2 | bDGlcNAc(1→2)aDMan(1→6)[bDGlcNAc(1→2)aDMan(1→3)]bDMan(1→4)bDGlcNAc(1→4) [aLFuc(1→6)]bDGlcNAc(1→)N17 |
| N61A | M5 | aDMan(1→6)[aDMan(1→3)]aDMan(1→6)[aDMan(1→3)]bDMan(1→4)bDGlcNAc(1→4)bDGlcNAc(1→)N61 |
| N74A | A3 | bDGlcNAc(1→6)[bDGlcNAc(1→2)]aDMan(1→6)[bDGlcNAc(1→2)aDMan(1→3)]bDMan(1→4)bDGlcNAc(1→4)bDGlcNAc(1→)N74 |
| N122A | M5 | aDMan(1→6)[aDMan(1→3)]aDMan(1→6)[aDMan(1→3)]bDMan(1→4)bDGlcNAc(1→4)bDGlcNAc(1→)N122 |
| N149A | FA2G2S1 | aDNeu5Ac(2→6)bDGal(1→4)bDGlcNAc(1→2)aDMan(1→6)<br>[bDGal(1→4)bDGlcNAc(1→2)aDMan(1→3)]bDMan(1→4)bDGlcNAc(1→4) [aLFuc(1→6)]bDGlcNAc(1→)N149 |
| N165A | FA2G2S2 | xaDNeu5Ac(2→6)bDGal(1→4)bDGlcNAc(1→2)aDMan(1→6)<br>[aDNeu5Ac(2→6)bDGal(1→4)bDGlcNAc(1→2)aDMan(1→3)]bDMan(1→4)bDGlcNAc(1→4) [aLFuc(1→6)]bDGlcNAc(1→)N165 |
| N234A | M8 | aDMan(1→2)aDMan(1→6)[aDMan(1→3)]aDMan(1→6)<br>[aDMan(1→2)aDMan(1→2)aDMan(1→3)]bDMan(1→4)bDGlcNAc(1→4)bDGlcNAc(1→)N234 |
| N282A | FA3 | bDGlcNAc(1→6)[bDGlcNAc(1→2)]aDMan(1→6)<br>[bDGlcNAc(1→2)aDMan(1→3)]bDMan(1→4)bDGlcNAc(1→4)[aLFuc(1→6)]bDGlcNAc(1→)N282 |

**Table S2.** mAbs and crystal structures used in the present study

| PDB ID | Antibody |
|---|---|
| 7C2L | 4A8[3] |
| 7CWS | FC05[4] |
| 7L2C | 2-51[5] |
| 7L2D | 1-87[5] |
| 7L2E | 4-18[5] |
| 7L2F | 5-24[5] |
| 7LAB | DH1052[6] |
| 7LQW | 2-17[5] |
| 7LXY | S2X333[7] |
| 7LXZ | S2L28[7] |
| 7LY2 | S2M28[7] |

**Table S3.** The predicted mAb-NTD binding free energy of 11 complexes excluding glycans' contribution

| PDB ID | Antibody | $\Delta G_{WT}$(kcal/mol) | $\Delta G_{R246I}$(kcal/mol) | $\Delta\Delta G^{a}$(kcal/mol) | $\Delta\Delta G/\Delta G_{WT}$ | R246(kcal/mol) | I246(kcal/mol) |
|---|---|---|---|---|---|---|---|
| 7L2F | 5-24 | -52.12±0.18 | -15.88±0.15 | 36.24 | -69.53% | -8.93±2.39 | -0.06±0.13 |
| 7C2L | 4A8 | -71.65±0.23 | -47.84±0.17 | 23.81 | -33.23% | -10.81±1.35 | -0.61±0.28 |
| 7LQW | 2-17 | -72.40±0.22 | -50.22±0.21 | 22.18 | -30.64% | -11.92±2.03 | -3.75±0.62 |
| 7L2C | 2-51 | -85.87±0.17 | -59.57±0.20 | 26.30 | -30.63% | -12.14±0.99 | -0.69±0.22 |
| 7LXZ | S2L28 | -49.05±0.13 | -25.06±0.25 | 23.99 | -48.91% | -2.73±0.58 | -1.38±0.29 |
| 7L2D | 1-87 | -88.89±0.19 | -85.61±0.21 | 3.28 | -3.69% | -9.93±1.49 | -1.09±0.33 |
| 7L2E | 4-18 | -83.66±0.23 | -84.69±0.19 | -1.03 | 1.23% | -0.85±0.59 | -1.35±0.56 |
| 7LAB | DH1052 | -31.53±0.23 | -33.67±0.30 | -2.14 | 6.79% | -0.04±0.02 | -0.00±0.00 |
| 7LXY | S2X333 | -63.62±0.26 | -60.00±0.27 | 3.62 | -5.69% | -3.48±3.63 | -3.20±0.67 |
| 7LY2 | S2M28 | -58.34±0.20 | -55.79±0.18 | 2.55 | -4.37% | -4.83±1.54 | -2.61±0.56 |
| 7CWS | FC05 | -44.11±0.20 | -55.34±0.17 | -11.23 | 25.46% | -6.14±3.88 | -0.57±0.26 |

a: $\Delta\Delta G = \Delta G_{R246I} - \Delta G_{WT}$

The $\Delta G$ was calculated based on 100-400 ns MD simulation trajectory. A total of 1500 snapshots evenly extracted from the 100-400 ns MD trajectory of each complex were used for MM/GBSA calculations.

**References**

1 L. Casalino, Z. Gaieb, J. A. Goldsmith, C. K. Hjorth, A. C. Dommer, A. M. Harbison, C. A. Fogarty, E. P. Barros, B. C. Taylor, J. S. McLellan, E. Fadda and R. E. Amaro, *ACS Cent Sci*, 2020, **6**, 1722-1734.

2 Y. Watanabe, J. D. Allen, D. Wrapp, J. S. McLellan and M. Crispin, *Science*, 2020, **369**, 330-333.

3 X. Chi, R. Yan, J. Zhang, G. Zhang, Y. Zhang, M. Hao, Z. Zhang, P. Fan, Y. Dong, Y. Yang, Z. Chen, Y. Guo, J. Zhang, Y. Li, X. Song, Y. Chen, L. Xia, L. Fu, L. Hou, J. Xu, C. Yu, J. Li, Q. Zhou and W. Chen, *Science*, 2020, **369**, 650-655.

4 N. Wang, Y. Sun, R. Feng, Y. Wang, Y. Guo, L. Zhang, Y. Q. Deng, L. Wang, Z. Cui, L. Cao, Y. J. Zhang, W. Li, F. C. Zhu, C. F. Qin and X. Wang, *Cell Res*, 2021, **31**, 101-103.

5 G. Cerutti, Y. Guo, T. Zhou, J. Gorman, M. Lee, M. Rapp, E. R. Reddem, J. Yu, F. Bahna, J. Bimela, Y. Huang, P. S. Katsamba, L. Liu, M. S. Nair, R. Rawi, A. S. Olia, P. Wang, B. Zhang, G. Y. Chuang, D. D. Ho, Z. Sheng, P. D. Kwong and L. Shapiro, *Cell Host Microbe*, 2021, **29**, 819-833.e817.

6 D. Li, R. J. Edwards, K. Manne, D. R. Martinez, A. Schafer, S. M. Alam, K. Wiehe, X. Lu, R. Parks, L. L. Sutherland, T. H. Oguin, 3rd, C. McDanal, L. G. Perez, K. Mansouri, S. M. C. Gobeil, K. Janowska, V. Stalls, M. Kopp, F. Cai, E. Lee, A. Foulger, G. E. Hernandez, A. Sanzone, K. Tilahun, C. Jiang, L. V. Tse, K. W. Bock, M. Minai, B. M. Nagata, K. Cronin, V. Gee-Lai, M. Deyton, M. Barr, T. Von Holle, A. N. Macintyre, E. Stover, J. Feldman, B. M. Hauser, T. M. Caradonna, T. D. Scobey, W. Rountree, Y. Wang, M. A. Moody, D. W. Cain, C. T. DeMarco, T. N. Denny, C. W. Woods, E. W. Petzold, A. G. Schmidt, I. T. Teng, T. Zhou, P. D. Kwong, J. R. Mascola, B. S. Graham, I. N. Moore, R. Seder, H. Andersen, M. G. Lewis, D. C. Montefiori, G. D. Sempowski, R. S. Baric, P. Acharya, B. F. Haynes and K. O. Saunders, *Cell*, 2021.

7 M. McCallum, A. De Marco, F. A. Lempp, M. A. Tortorici, D. Pinto, A. C. Walls, M. Beltramello, A. Chen, Z. Liu, F. Zatta, S. Zepeda, J. di Iulio, J. E. Bowen, M. Montiel-Ruiz, J. Zhou, L. E. Rosen, S. Bianchi, B. Guarino, C. S. Fregni, R. Abdelnabi, S. C. Foo, P. W. Rothlauf, L. M. Bloyet, F. Benigni, E. Cameroni, J. Neyts, A. Riva, G. Snell, A. Telenti, S. P. J. Whelan, H. W. Virgin, D. Corti, M. S. Pizzuto and D. Veesler, *Cell*, 2021, **184**, 2332-2347.e2316.